Mineralogical Magazine, October 2004, Vol. 68(5), pp. 801–811

Infrared and Raman spectra of $ZrSiO_4$ experimentally shocked at high pressures

A. Gucsik[1], M. Zhang[2,*], C. Koeberl[1], E. K. H. Salje[2], S. A. T. Redfern[2] and J. M. Pruneda[2]

[1] Institute of Geological Sciences, University of Vienna, Althanstrasse 14, A-1090 Vienna, Austria
[2] Department of Earth Sciences, University of Cambridge, Downing Street, Cambridge CB2 3EQ, UK

ABSTRACT

Zircon- and reidite-type $ZrSiO_4$ produced by shock recovery experiments at different pressures have been studied using infrared (IR) and Raman spectroscopy. The ν_3 vibration of the SiO_4 group in shocked natural zircon shows a spectral change similar to that seen in radiation-damaged zircon: a decrease in frequency and increase in linewidth. The observation could imply a possible similar defective crystal structure between the damaged and shocked zircon. The shock-pressure-induced structural phase transition from zircon ($I4_1/amd$) to reidite ($I4_1/a$) is proven by the occurrence of additional IR and Raman bands. Although the SiO_4 groups in both zircon- and reidite-$ZrSiO_4$ are isolated, the more condensed scheelite gives rise to Si−O stretching bands at lower frequencies, suggesting a weakening of the bond strength. Low-temperature IR data of the reidite-type $ZrSiO_4$ show an insignificant effect of cooling on the phonon modes, suggesting that the structural response of reidite to cooling-induced compression is weak and its thermal expansion is very small.

Keywords: $ZrSiO_4$, zircon, reidite, scheelite structure, high pressure, phase transition, infrared spectroscopy, Raman spectroscopy, metamictization.

Introduction

Zircon ($ZrSiO_4$) is widely used in the ceramic, foundry and refractory industries owing to its high thermal conductivity, chemical stability and ability to accommodate a number of dopant ions. Recently, it has been the subject of extensive research because it is commonly used in U/Pb radiometric age dating and it is also among several crystalline phases currently under consideration for the immobilization and disposal of high-actinide radioactive wastes (Anderson *et al*., 1993; Ewing *et al*., 1995; Weber *et al*., 1996).

Zircon has a tetragonal structure with space group D_{4h}^{19} or $I4_1/amd$ (a = 6.607 Å and c = 5.981 Å) (e.g. Hazen and Finger, 1979). The ideal structure consists of chains of edge-sharing, alternating SiO_4 tetrahedra and ZrO_8 triangular dodecahedra extending parallel to the crystallographic c axis. Under compression, zircon undergoes a structural phase transition to form a scheelite-structure phase (space group $I4_1/a$, a = 4.734 Å and c = 10.51 Å) with an increase in density of 9.9% (Reid and Ringwood, 1969; Liu, 1979; Mashimo *et al*., 1983; Kusaba *et al*., 1985, 1986). The scheelite-structure phase has recently been discovered in naturally occurring samples (Glass and Liu, 2001) and the mineral was named reidite after Alan Reid, who first produced the phase in the laboratory (Glass *et al*., 2002). The pressure at which the transition takes place is reported to be ~30 GPa for natural zircon in shock experiments at room temperature (e.g. Kusaba *et al*., 1985). A recent *in situ* study showed that, at room temperature, the onset of the phase transition is at a pressure of 20 GPa in synthetic pure $ZrSiO_4$ (van Westrenen *et al*., 2004). The transition pressure is also affected by temperature as heating leads to lowering of the transition pressure (Reid and Ringwood, 1969). Due to the importance of shock metamorphism in geology and mineralogy, the effects of pressure-induced

* E-mail: mz10001@esc.cam.ac.uk
DOI: 10.1180/0026461046850220

shock on zircon and characterization of the scheelite-structure $ZrSiO_4$ have attracted considerable attention (e.g. Bohor *et al*., 1993; Knittle and Williams, 1993; Leroux *et al*., 1999; Glass *et al*., 2002; Gucsik *et al*., 2002, 2004; Farnan *et al*., 2003; Ono *et al*., 2004; Reimold *et al*., 2002; Ríos and Boffa-Ballaran, 2003; Scott *et al*., 2002; van Westrenen *et al*., 2004).

In this study, we aim to provide a better understanding of shocked $ZrSiO_4$, especially scheelite-type $ZrSiO_4$ from their IR and Raman spectra. Although some previous reports have shown vibrational spectra of the scheelite phase (Kusaba *et al*., 1985; Knittle and Williams, 1993; Gucsik *et al*., 2002, 2004; Scott *et al*., 2000; van Westrenen *et al*., 2004), these measurements were conducted in limited frequency regions, and the band positions and number of bands obtained in different studies are inconsistent. Our second aim was related to understanding α-decay damage in zircon. It has been documented that, due to radioactive decay of naturally occurring radionuclides and their daughter products in the ^{238}U, ^{235}U and ^{232}Th decay series, the crystal structure of natural zircon can be heavily damaged over geological times, resulting in an aperiodic or amorphous state – the metamict state (Ewing, 1994; Weber *et al*., 1998; Salje *et al*., 1999). Extensive studies in the past decade have focused on the effect of radiation on the physical and chemical properties of zircon, on the structures of the metamict state and on the recovery of the damaged structure at high temperatures (see Weber *et al*., 1998 and Ewing *et al*., 2003 for reviews). One important scientific issue is what happens at the atomic level during metamictization, and what the roles of the α particle and the recoil in the damage process are. It is commonly believed that during α-decay radiation damage, the energetic recoil (70−100 keV) transfers most of its energy in collisions (Weber *et al*., 1998). This probably leads to an ultra-fast (in the order of ps) high-temperature process in the displacement cascades that could melt the material (e.g. Miotello and Kelly, 1997; Meldrum *et al*., 1998) and the melts could quench very quickly. The process might involve local high stress and/or pressure. In addition, a recent computer simulation has proposed that radiation damage in zircon leads to polymerization (formation of direct Si−O−Si linkages), shear deformation and the formation of highly dense regions (Trachenko *et al*., 2002), which might also be associated with local high pressures. As one of the most extensively investigated materials in the study of metamictization, zircon has a relatively simple structure and its chemical and physical properties are well understood. We wish to investigate the possible spectral similarities or differences between radiation-damaged zircon and high-pressure shocked zircon for the purpose of illuminating the metamictization process.

Experimental methods

The zircon samples used in this study originated from Sri Lanka and the starting material showed the ν_3 (SiO_4) Raman band at 1006.7 cm^{-1} with a measured width of 3.6 cm^{-1} (the value is measured at the full width at half maximum – FWHM), which indicates that the crystal is crystalline and lacks α-decay damage. The crystal was cut into thin plates ~1 mm thick, parallel and at 45º to their crystallographic *c* axes. Shock recovery experiments were performed (shock pressures between 20 and 80 GPa) on such plates using the shock reverberation technique at the Ernst-Mach-Institute, Germany (e.g. Deutsch and Schärer, 1990; Stöffler and Langenhorst, 1994). The samples had previously been investigated by electron microscopy, and micro-Raman spectroscopy (Leroux *et al*., 1999; Gucsik *et al*., 2002, 2004). The samples were re-examined by IR, FT-Raman and micro-Raman spectroscopy in the present study to address the issues described in earlier sections and to improve the data quality. In addition to small crystals, impact-induced tiny gains or powders from the shocked samples were also measured by micro-Raman and powder absorption spectroscopy. The IR powder pellet technique reported by Zhang and Salje (2001) was employed in the powder absorption measurements. Due to the limitation of the sample powders, the IR powder absorption measurements were carried out only on the 80 GPa sample and a crystalline sample from Sri Lanka. CsI powder was used as matrix material. The sample/matrix ratio was 1:300. Sample powders were thoroughly mixed with the matrix material. 300 mg of the mixture were pressed into 13 mm discs under vacuum. The sample pellets were measured within 12 h of creation to avoid possible reactions between the sample and the matrix material. Infrared reflectance and Raman measurements were also made on small crystal grains under unpolarized conditions because of the small sizes of the materials.

Powder IR spectra between 150 and 2500 cm^{-1} were recorded using a Bruker 113v FT-IR spectrometer (see Zhang and Salje, 2001 for detailed information on instrumentals). Reflectance spectra between 650 and 5000 cm^{-1} were recorded at an almost normal incident condition using an IR microscope equipped with a mapping stage and attached to a Bruker IFS 66v FT-IR spectrometer. The beam size was 80 μm. A liquid-nitrogen-cooled MCT detector, coupled with a KBr beamsplitter and a Globar source were used. The spectra were averaged by 512 scans with a spectral resolution of 2 cm^{-1}. Gold mirrors were used as the reference for the reflectance measurements. For low-temperature measurements, a closed-cycle liquid-helium cryostat (LEYBOLD), equipped with KRS5 and polyethylene windows, was used. Two Si-diode temperature sensors (LakeShore, DT-470-DI-13), well calibrated by their manufacturers, were used in the cryostat. One was used to control the cryostat and the other for measuring the sample temperature. The temperature stability was better than 1 K.

Conventional Raman spectra were collected with a free-sample-space LabRam micro-Raman spectrometer. A 623 nm Ne-He laser was used for the excitation. A CCD detector, a grating (1800 grooves/mm), and a 50× ultra-long working-distance objective and a 100× objective were coupled with a free space microscope. The instrumental resolution of 3.5 cm^{-1} was used. In order to check any possible laser-induced fluorescence, FT-Raman spectra were also recorded at room temperature using a Bruker IFS 66v spectrometer adapted with a Bruker FRA 106 FT-Raman accessory. A silicon-coated calcium fluoride beam-splitter and radiation of 1064 nm from a Nd:YAG laser were used for the excitation laser. A liquid-nitrogen-cooled, high-sensitivity Ge detector was used. The FT-Raman spectra were recorded with a resolution of 2 cm^{-1}, a laser power of ~100 mW and a back-scattering geometry.

Results and discussion

IR spectra

Unpolarized reflectance spectra (650–1300 cm^{-1}) of $ZiSiO_4$ shocked at different pressures are shown in Fig. 1*a*. The strong reflection features between 800 and 1100 cm^{-1} are due to Si–O stretching bands in zircon and reidite. The pressure-induced phase transition from zircon (with space group $I4_1/amd$) to reidite (with space group $I4_1/a$) is characterized by the spectral differences between untreated zircon and the samples shocked at 20, 38, 40, 60 and 80 GPa. The general similarities in the spectra of these samples shocked at and above 38 GPa imply that these samples consist mainly of reidite, although small volumes of zircon might remain in some of the samples as a result of heterogeneous compression across the crystal.

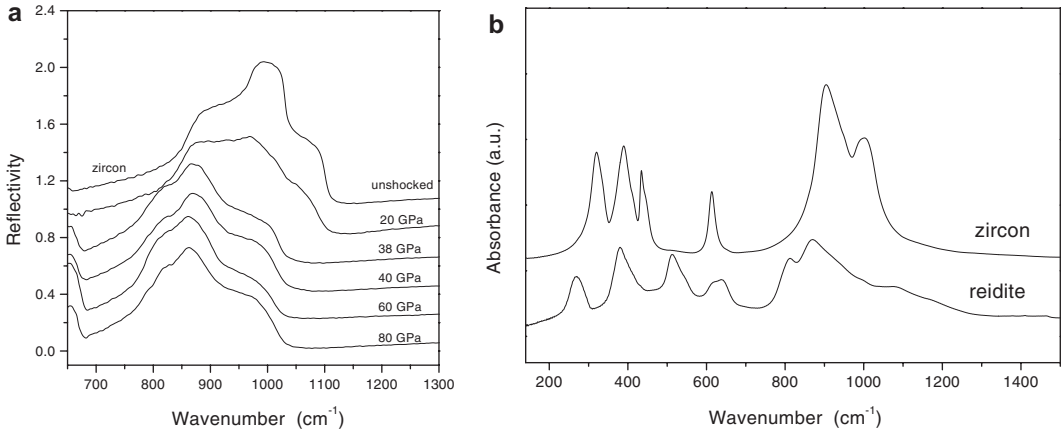

FIG. 1. (*a*) Micro-IR reflectance spectra (650–1300 cm^{-1}) of the untreated zircon and the samples shocked at different pressures. Spectral differences between the untreated zircon and the samples shocked at and above 38 GPa are mainly due to the change of crystal symmetry during the zircon–reidite phase transition. (*b*) Comparison of IR powder absorption spectra (150–1500 cm^{-1}) of zircon and the sample shocked at 80 GPa containing mainly reidite phase.

The differences between the IR features for zircon and reidite $ZrSiO_4$ are attributed to the symmetry changes at the phase transition as well as differences in bond lengths. Powder IR absorption spectra of reidite and zircon are shown in Fig. 1*b*; the former is taken from the sample shocked to 80 GPa. Although both materials are tetragonal, the denser phase (i.e. the scheelite-structure phase) is characterized by a shift of the Si–O stretching bands to lower wavenumbers. We noted the appearance of a feature near 1080 cm^{-1} in the 80 GPa sample. The wavenumber of its position is >200 cm^{-1} higher than these of the bands near 813 and 871 cm^{-1}. It is difficult to attribute the frequency difference to symmetry-induced band splitting of the Si–O stretching bands of scheelite $ZrSiO_4$, because only two IR-active bands of the scheelite phase are expected in this frequency region. Furthermore, a frequency of 1080 cm^{-1} is not consistent with the Si–O stretching band of zircon (Fig. 1*b*). Low-temperature data (see below) revealed additional weak absorption bands near this 1080 cm^{-1} band. Therefore, these features are unlikely to be associated with reidite, but probably due to a high-pressure-induced amorphous phase or possibly due to SiO_2 resulting from decomposition of $ZrSiO_4$.

We noted that the sample shocked at 20 GPa (Fig. 1*a*) exhibits broad and less distinct reflectance signals, although Raman data (see below) indicate that the sample essentially has the zircon structure. We consider that the spectral changes are associated with structural distortion and strain caused by high-pressure shocking. Transmission electron microscopy (TEM) data (Leroux *et al*., 1999; Reimold *et al*., 2002) show evidence of shock-induced deformation and the formation of dislocations. The importance of our finding is that line broadening seen in natural zircon could be caused by shock-induced defects and structural deformation.

The IR powder absorption spectrum of the sample shocked at 80 GPa was also recorded at low temperatures to investigate the thermal evolution of the phonon modes of the scheelite phase and also to further study the observed IR features, as vibrational bands generally sharpen at low temperatures. The effect of cooling on the phonon modes of the scheelite phase is weak (Fig. 2). For instance, the band at 868 cm^{-1} (at room temperature), which is considered to be due to a Si–O stretching vibration, shifted to 871 cm^{-1} at 20 K. The other IR bands showed small or undetectable changes in frequency. This indicates that the scheelite phase of $ZrSiO_4$ has a very weak thermal expansion and the structural compression caused by the cooling is weak. The data from cooling measurements resolved certain spectral features. At 20 K, the sample showed clearly local maxima near 1000, 1080 and 1180 cm^{-1}, which are too high in frequency to be due to isolated SiO_4 groups.

Raman spectra

Room-temperature micro-Raman spectra of zircon and reidite-$ZrSiO_4$ are shown in Fig. 3*a*,*b*. The spectrum of zircon exhibits a strong ν_3 band (anti-symmetric stretching of the SiO_4 group) near 1008 cm^{-1}, which has been shown to have B_{1g} symmetry (Dawson *et al*., 1971). The band near 974 cm^{-1} is assigned as a Si–O stretching band (ν_1, symmetric stretching) with A_{1g} symmetry. Other relatively intense Raman bands of zircon are located in low-frequency regions, and they are attributed to bending vibrations of SiO_4 groups and external bands associated with SiO_4 group motions with respect to Zr atoms and motions of Zr atoms (Dawson *et al*., 1971). The structural transition from zircon (with space group $I4_1/amd$) to reidite (with space group $I4_1/a$) is proven by a systematic change of Raman features (Fig. 3*b*). The scheelite-structure $ZrSiO_4$ (e.g. the sample shocked to 80 GPa) clearly shows more Raman bands due to its lower crystal symmetry. Just as with the IR data (Fig. 1*b*), the relatively strong Si–O stretching bands shift to lower frequency in this structure. FT-Raman spectra of shocked samples

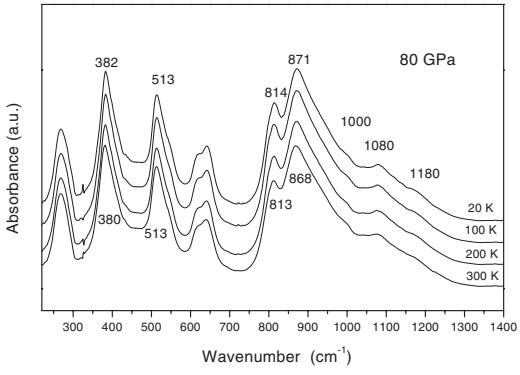

FIG. 2. Temperature evolution (between 20 and 300 K) of absorption spectra of the scheelite phase (sample shocked at 80 GPa).

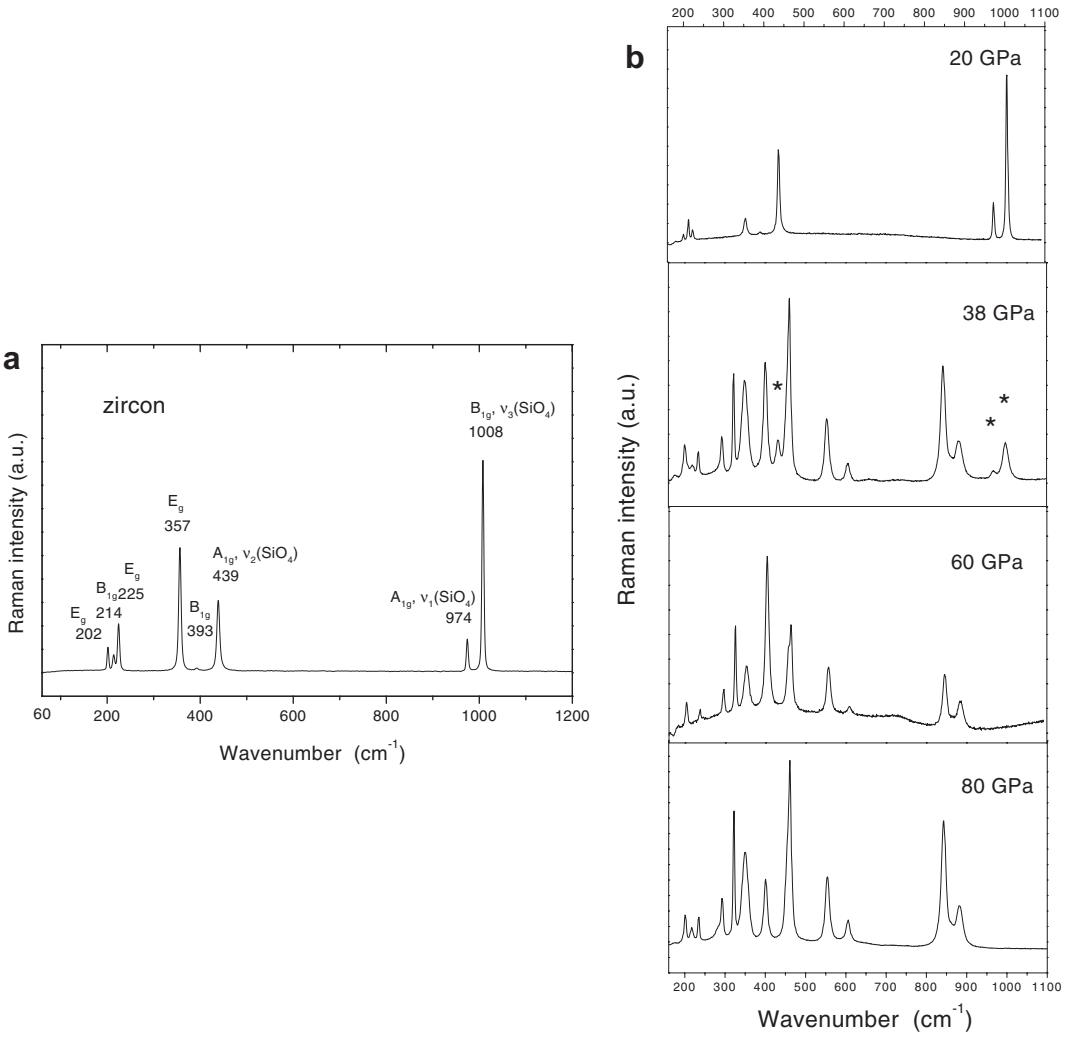

FIG. 3. Raman spectra of (*a*) zircon; (*b*) samples shocked at 20, 38, 60 and 80 GPa. The 20 GPa sample still has the zircon structure.

were also recorded to check laser-induced fluorescence. The FT-Raman spectra are essentially similar to those from conventional Raman spectroscopy, in terms of the number of bands and their frequencies, although FT-Raman spectra of the shocked samples exhibit a relatively high background at low frequencies. This confirms the reliability of the micro-Raman data. We found that the Raman bands near 966 and 1000 cm^{-1} are not Raman bands of scheelite-structure $ZrSiO_4$. Although they were observed in some samples shocked at lower shock pressures, they did not occur in all areas sampled and they could hardly be seen in the powder sample shocked to 80 GPa. We believe that they originate from remaining untransformed zircon domains as suggested by some previous studies (e.g. van Westrenen *et al*., 2004; Gucsik *et al*., 2004). Gucsik *et al*. (2004) reported that Raman spectra of the naturally shock-deformed zircon crystals from the Ries impact structure (Germany) represent zircon-structure material, whereas a sample from the shock-metamorphic (suevite) rock shows additional peaks with relatively high peak intensities, which are indicative of the presence of the scheelite-type structure of

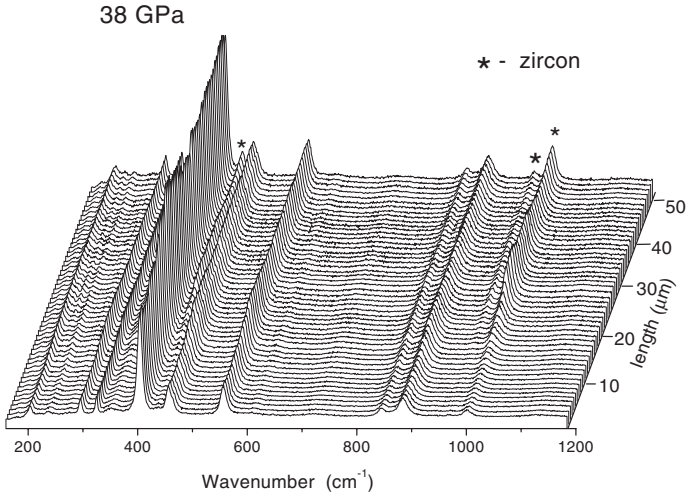

FIG. 4. Raman spectra from mapping measurements on the sample shocked at 38 GPa. The data show that zircon and reidite coexist in this sample. The bands marked by asterisks are due to the zircon remnants

$ZrSiO_4$ (reidite) with zircon-structure relics. They concluded that the naturally shock-deformed zircons might be related to the low-shock regime (<30 GPa), and do not represent the same shock stages as indicated by whole-rock petrography.

Our results suggest that zircon and reidite coexist in samples shocked at and above 38 GPa (although the volume of zircon domains is very limited in the sample shocked to 80 GPa, they can still be detected in several regions). This is associated with the heterogeneities of the shock, which causes some regions to remain structurally untransformed. The sample shocked from 38 GPa was further examined using a micro-Raman mapping technique, in order to gain some understanding of the degree of the heterogeneities. The mapping data were recorded in a grid over an area of 50×50 μm with a beam size of ~1 μm and a step of 1 μm. The results show systematic variations of the intensity of Raman bands attributed to zircon in a scale of 20−30 μm, indicating that the amount of the untransformed zircon phase changes across the sample. A typical spectrum evolution along one direction of the mapped area is shown in Fig. 4. The bands marked by asterisks are due to the zircon remnants. The different Raman intensity of these bands along the measured length reflects the heterogeneity of the shock pressure. The intensity ratio between the strong band near 884 cm^{-1} in the scheelite phase and the ν_3 band in zircon is plotted in Fig. 5. The two bands were chosen because they are both due to Si-O stretching vibrations. The ratio reflects the relative contents of the two phases. The data also indicate that the untransformed zircon remnants are of the order of sub-micro or nanometers in scale, i.e. smaller than the laser beam size (~1 μm) used. Our observation of coexistence of the phases in shocked samples is consistent with the work of Leroux *et al*. (1999), who found that at 40 GPa shock pressure, the sample was partly transformed from the zircon to the scheelite structure. It is also consistent with XRD measurements at hydrostatic pressures >20 GPa in pure $ZrSiO_4$ (van Westrenen *et al*., 2004). We also found that the

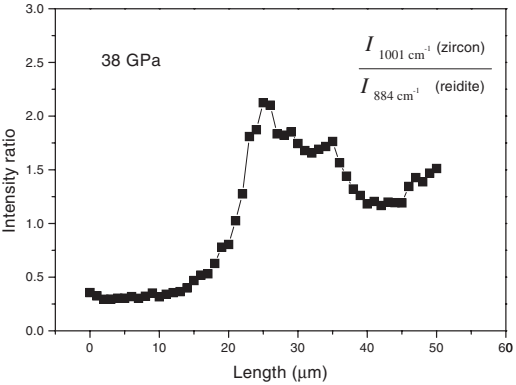

FIG. 5. Intensity ratio between the ν_3 band near 1001 cm^{-1} of the zircon remnants and the 884 cm^{-1} band of the scheelite phase (38 GPa sample). The lines are visual guides.

shock-induced sample powders (see earlier sections for more details) appear to have experienced more significant impact than these crystals shocked to the same pressures, because much weaker micro-Raman signals of the zircon phase were commonly recorded in the impact-induced powders, suggesting a better transformation of zircon into reidite.

One of the interesting observations in the present study is that the internal mode frequencies of the SiO_4 tetrahedra generally dropped to lower values in the scheelite phase as described earlier (for instance, the IR-active Si−O stretching bands in zircon near 980 and 880 cm^{-1} shift to 868 and 813 cm^{-1} in the scheelite phase). This change is associated with the modification of local configurations of the sample through the transition. In particular, the frequency values for the Raman Si−O stretching vibrations between near 800 and 890 cm^{-1} in reidite indicate a change of the Si−O bond strength caused by the phase transition. The change can be estimated by calculating the change associated with force constant k, since under the harmonic approximation a phonon frequency is given by:

$$\nu = \frac{1}{2\pi c}\sqrt{\frac{k}{m}} \qquad (1)$$

where k, m and c are force constant, reduced mass and the velocity of light, respectively. The change of force constant can be extracted from

$$k_{scheelite}/k_{zircon} \approx \nu_{scheelite}^{2}/\nu_{zircon}^{2} \qquad (2)$$

Thus, the relative change in the force constant, which is directly related to the change in bond strength, can be measured through the square of their frequency ratio. This approach shows that there is a surprising ~11% decrease in the Si−O bond strength (for the above IR bands) during the phase transition from zircon to the scheelite structure. This change may have several origins: an increase in the bond length, a change in electron density function or a charge transfer involving O and Si, or O and Zr or a combination of all these factors. Powder XRD data have shown a small (<1%) increase in the SiO_4 tetrahedral bond length when zircon is shocked-transformed into the scheelite-type structure (Kusaba *et al*., 1986). Therefore, charge transfer might play a significant role in the change of phonon frequencies. We noted that although the untreated zircon samples are light yellow, the shocked samples are commonly dark brown. This could indicate that during the structural transition there is a change of electronic structure. In fact, charge transfer was observed in the zircon-scheelite transition of other materials (Jayaraman *et al*., 1987; Duclos *et al*., 1989). As a result, the density increase at the zircon-reidite structural transition is expected to be associated with not only a more efficient packing of the coordination polyhedra and the elimination of a structural hole in the zircon-type structure (Stubican and Roy, 1963; Reid and Ringwood, 1969), but also significant changes related to the SiO_4 group and its local environment.

Our Raman measurements reveal, apart from the reidite phase, an unexpected phase in some samples shocked to pressures >40 GPa, which can be associated with the extra feature seen in our IR spectra. The phase appeared in only some sampled regions and showed bands near 212, 272, 383 and 586 cm^{-1} (their wavenumbers vary slightly from sampling areas to areas), which are not due to characteristic bands of either zircon or reidite. These features were not seen in the starting material. This implies that its occurrence is not due to potential original inclusions, but associated with the high-pressure process. The signals appeared in both FT-Raman and conventional Raman spectra, suggesting that it is not associated with laser-induced fluorescence. We noted that in previous studies (Liu, 1979; Kusaba *et al*., 1985), high-pressure-induced decomposition was reported, as proven by signals corresponding to ZrO_2. However, the band frequencies of the additional phase match neither the characteristic bands of monoclinic, tetragonal nor cubic ZrO_2 (Carlone, 1992; Kim *et al*., 1993; Hirata *et al*., 1994; Zhang *et al*., 2000*a*,*b*), nor those of SiO_2 glass and coesite (a high-pressure phase of SiO_2), although the bands at 212 and 586 cm^{-1} have frequencies close to those of two Raman bands (near 231 and 589 cm^{-1}) of stishovite, a high-pressure polymorph of SiO_2. At this stage we are unable to clarify the nature of the phase, but it could be connected to the additional phase observed in a recent electron microscopy study (Leroux *et al*., 1999).

Effect of shock pressure on phonon modes of zircon-type $ZrSiO_4$

One of the important observations in this study is the effect of high-pressure shock on the frequency and width of zircon phonons, i.e. the shocked zircon phase shows some variations in post-shock

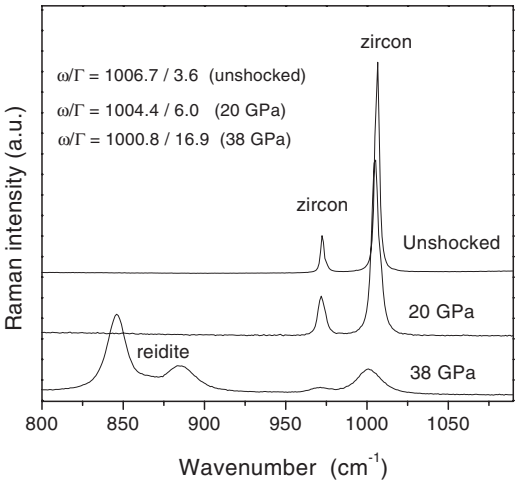

FIG. 6. The effect of high-pressure shock on the ν_3 vibration (SiO_4) in zircon. The values of the frequency (ω in cm^{-1}) and measured linewidth (γ in cm^{-1}) of the ν_3 vibration are given at different pressures.

peak profiles. As shown in Fig. 6, Raman bands (between 970 and 1100 cm^{-1}) of the remaining zircon phase in shocked samples exhibit clear broadening upon increasing shock pressure. For instance, in the sample shocked at 20 GPa the ν_3 vibration of the SiO_4 group has an averaged frequency of ~1004 cm^{-1} and a mean linewidth (measured full width at half magnitude) of ~6 cm^{-1}, although the measured frequency and width in the starting material are 1006.7 cm^{-1} and 3.6 cm^{-1}, respectively. As shown by IR (Fig. 1*a*) and Raman data (Figs 3*b*, 6), the sample shocked at 20 GPa still has the zircon structure. The broadening is more significant in the 38 GPa sample, which shows a bandwidth of ~17 cm^{-1}, four times larger than that of the starting material. The frequency decrease with increasing shock pressure shown in Fig. 6 appears opposite to the pressure-induced increase of the frequency reported by Knittle and Williams (1993). But the difference is mainly due to different experimental methods, as the latter authors' data were obtained through *in situ* high-pressure measurements, whereas our results were from shocked samples. The decompressed sample in the Knittle and Williams study (from *in situ* measurements up to 38 GPa) showed a band near 1001 cm^{-1}, which was incorrectly considered as a characteristic mode of scheelite-structure $ZrSiO_4$. The change of spectral parameters in the present study is related to the post-shock 'damage' that is retained in the shocked sample, whereas the increase of frequency in *in situ* experiments is more closely associated with dynamic effects of compression on the structure of zircon. The change in the frequency and width of the ν_3 band is probably due to pressure-induced deformation, local defects and strains. Plastic deformation was observed in a sample pressurized to 20 GPa, and is characterized by a high density of straight dislocations in glide configuration (Leroux *et al*., 1999). According to Leroux *et al*. (1999), the large density of dislocations at crack tips shows that the plastic deformation was initiated by a micro-cracking process. Our data from the Raman mapping measurements indicate that the measured frequency and width of the zircon remnants vary from area to area in the shocked sample. In order to understand the spatial variation better, the data shown in Fig. 4 were curve-fitted to extract the spectral parameters. Figure 7*a*,*b* shows the variation in frequency and

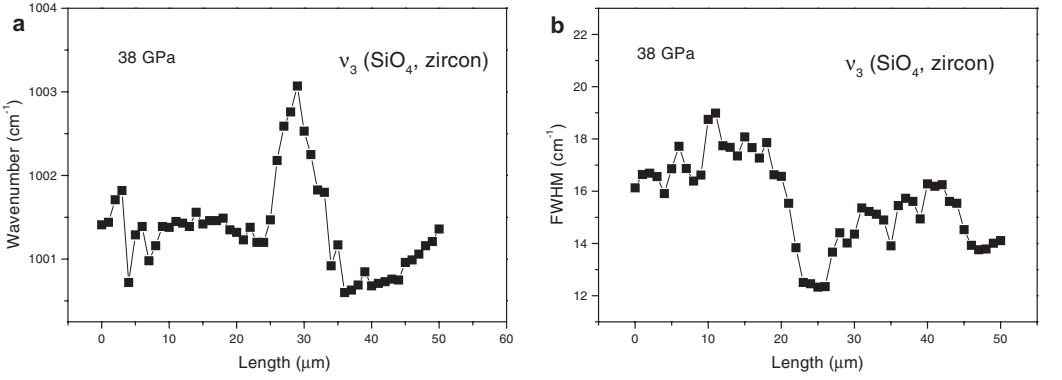

FIG. 7. Spectral parameters of the ν_3 band near 1001 cm^{-1} of the zircon remnants (38 GPa sample) as a function of length: (*a*) frequency, and (*b*) measured width. The lines are visual guides.

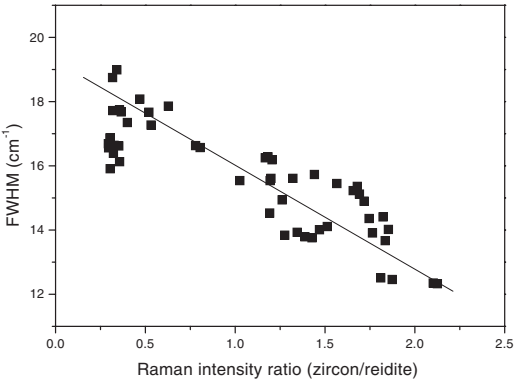

FIG. 8. The width of the ν_3 band near 1001 cm^{-1} of the zircon remnants (38 GPa sample) as a function of the Raman intensity ratio between the ν_3 band of zircon and the 884 cm^{-1} band of the scheelite phase. The line is a visual guide.

width of the Raman ν_3 along a 50 μm trajectory. The regions that show a broader linewidth are interpreted as having undergone higher local pressures, and having more defects and large local strains. The different width and frequency values in the mapped region further confirm the heterogeneity of the pressure impact. The simple relationship between the width and amount of the zircon remnants in the shocked sample is shown by plotting the width as a function of the Raman intensity ratio between the ν_3 band of zircon and the 884 cm^{-1} band of scheelite phase in Fig. 8. It is clear that regions with higher values of width are more likely to have undergone a higher-pressure shock as fewer zircon remnants are found. Furthermore, the correlation shown in Fig. 8 is consistent with the observation shown in Fig. 6. One of the potential applications of our finding is that Raman measurements provide a means to estimate the shock pressure through the mean phonon linewidth. But other facts could make this correlation more complex, e.g. metamictization in natural zircon.

The impact of metamictization on the phonon frequency and width for zircon is similar to the impact of shock pressure in the same material. In recent Raman studies of the effect of radiation damage, it has been found that α-decay radiation causes a systematic variation of band frequency and width (e.g. Nasdala *et al*., 1995; Wopenka *et al*., 1996; Zhang *et al*., 2000*a*,*b*; Geisler *et al*., 2001b; Palenik *et al*., 2003). This is clearly demonstrated by the behaviour of the ν_3 (SiO_4) band near 1008 cm^{-1}, which shifts to ~995 cm^{-1} with an increase in linewidth to 20–30 cm^{-1} for natural metamict zircon. Data from extensive annealing experiments have also shown that the band parameters can be systematically affected by thermal annealing (Zhang *et al*., 2000*a*; Geisler *et al*., 2001*b*) and by hydrothermal alteration (Geisler *et al*., 2001*a*). The peak profile of this Raman ν_3 band has been used to predict the thermal history of zircon, and hence its host rocks. Nasdala *et al*. (2001) used the width to estimate the possible thermal history of natural zircons, whereas Geisler *et al*. (2001*b*) proposed the use of both the width and frequency to trace potential thermal alterations. Although high-pressure shock and metamictization are two processes with distinctly different origins, the changes in frequency and linewidth are most likely to be associated with defects in both cases. The similarities between the two processes, shown by the phonon modes of zircon, could reflect similar local changes and defective crystal structures "seen" by the phonons. However, the absence of the characteristic bands of scheelite-type $ZrSiO_4$ in metamict zircon indicates that the possible high pressure extremes involved in radiation damage during atomic displacements in the cascades must be <20 GPa, because around this pressure the zircon-reidite transition starts to take place at room temperature (e.g. van Westrenen *et al*., 2004). The real pressure associated with the cascades could be significantly lower than this value, as the radiation self-damage process is associated with high effective temperatures and experiments have shown that increasing temperature lowers the zircon-reidite transition pressure dramatically (Reid and Ringwood, 1969; Liu, 1979).

Acknowledgements

The authors would like to thank Ansgar Greshake for providing the shocked samples used in this study. Financial assistance from the Paneth Trust and British Nuclear Fuels Limited (BNFL) is gratefully acknowledged. The manuscript benefited from reviews by W. van Westrenen and an anonymous reviewer.

References

Anderson, E.B., Burakov, B.E. and Vasiliev, V.G. (1993) Creation of a crystalline matrix for actinide waste at Khlopin Radium Institute. *Proceedings of Safe Waste*, *93*, **2**, 29–33.

Bohor, B.F., Betterton, W.J. and Krogh, T.E. (1993) Impact-shocked zircons – Discovery of shock-induced textures reflecting increasing degrees of shock metamorphism. *Earth and Planetary Science Letters*, **119**, 419–424.

Carlone, C. (1992) Raman spectrum of zirconia-hafnia mixed crystals. *Physical Review B*, **45B**, 2079–2084.

Dawson, P., Hargreave, M.M. and Wilkinson, G.F (1971) The vibrational spectrum of zircon ($ZrSiO_4$). *Journal of Physics C: Solid State Physics*, **4**, 240–256.

Deutsch, A. and Schärer, U. (1990) Isotope systematics and shock-wave metamorphism: I. U-Pb in zircon, titanite, and monazite, shocked experimentally up to 59 GPa. *Geochimica et Cosmochimica Acta*, **54**, 3427–3434.

Duclos, S.J., Jayaraman, A., Espinosa, G.P., Cooper, A.S. and Maines, R.G. (1989) Raman and optical-absorption studies of the pressure-induced zircon to scheelite structure transition in $TbVO_4$ and $DyVO_4$. *Journal of Physics and Chemistry of Solids*, **50**, 769–775.

Ewing, R.C. (1994) The metamict state: 1993 – the centennial. *Nuclear Instruments and Methods in Physics Research*, **B91**, 22–29.

Ewing, R.C., Lutze, W. and Weber, W. J. (1995) Zircon – a host-phase for the disposal of weapons plutonium. *Journal of Materials Research*, **10**, 243–246.

Ewing, R.C., Meldrum, A., Wang, L.M., Weber, W.J. and Corrales, L.R. (2003) Radiation effects in zircon. Pp. 387–425 in: *Zircon* (J.M. Hanchar and P.W.O. Hoskin, editors). Reviews in Mineralogy and Geochemistry, **53**, Mineralogical Society of America, Washington, D.C.

Farnan, I., Balan, E., Pickard, C.J. and Mauri, F. (2003) The effect of radiation damage on the local structure in the crystalline fraction of $ZrSiO_4$: Investigating the ^{29}Si NMR response to pressure in zircon and reidite. *American Mineralogist*, **88**, 1663–1667.

Geisler, T., Ulonska, M., Schleicher, H., Pidgeon, R.T. and van Bronswijk, W. (2001*a*) Leaching and differential recrystallization of metamict zircon under experimental hydrothermal conditions. *Contributions to Mineralogy and Petrology*, **141**, 53–65.

Geisler, T., Pidgeon, R.T., van Bronswijk, W. and Pleysier, R. (2001*b*) Kinetics of thermal recovery and recrystallization of partially metamict zircon: a Raman spectroscopic study. *European Journal of Mineralogy*, **13**, 163–1176.

Glass, B.P. and Liu, S. (2001) Discovery of high-pressure $ZrSiO_4$ polymorph in naturally occurring shock-metamorphosed zircons. *Geology*, **29**, 371–373.

Glass, B.P., Liu S. and Leavens, P.B. (2002) Reidite: An impact-produced high-pressure polymorph of zircon found in marine sediments. *American Mineralogist*, **87**, 562–565.

Gucsik, A., Koeberl, C., Brandstätter, F., Reimold, W.U. and Libowitzky, E. (2002) Cathodoluminescence, electron microscopy, and Raman spectroscopy of experimentally shock-metamorphosed zircon. *Earth and Planetary Science Letters*, **202**, 495–509.

Gucsik, A., Koeberl, C., Brandstätter, F., Libowitzky, E. and Reimold, W.U. (2004) Cathodoluminescence, electron microscopy, and Raman spectroscopy of experimentally shock metamorphosed zircon crystals and naturally shocked zircon from the Ries impact crater. Pp 281–322 in: *Cratering in Marine Environments and on Ice* (H. Dypvik, M. Burchell and Ph. Claeys, editors). Springer-Verlag, Heidelberg, Germany.

Hazen, R.M. and Finger, L.W. (1979) Crystal structure and compressibility of zircon at high pressure. *American Mineralogist*, **64**, 157–161.

Hirata, T., Asari, E. and Kitajima, M. (1994) Infrared and Raman spectroscopic studies of ZrO_2 polymorphs doped with Y_2O_3 or CeO_2. *Journal of Solid State Chemistry*, **110**, 201–207.

Jayaraman, A., Kourouklis, G.A., Espinosa, G.P., Cooper, A.S., Vanuitert, L.G. (1987) A high-pressure Raman-study of yttrium vanadate (YVO_4) and the pressure-induced transition from the zircon-type to the scheelite-type structure. *Journal of Physics and Chemistry of Solids*, **48**, 755–759.

Kim, D.J., Jung, H.J. and Yang, I.S. (1993) Raman spectroscopy of tetragonal zirconia solid solutions. *Journal of the American Ceramic Society*, **76**, 2106–2108.

Knittle, E. and Williams, Q. (1993) High-pressure Raman-spectroscopy of $ZrSiO_4$ – Observation of the zircon to scheelite transition at 300 K. *American Mineralogist*, **78**, 245–252.

Kusaba, K., Syono, Y., Kikuchi, M. and Fukuoka, K. (1985) Shock behaviour of zircon – phase transition to scheelite structure and decomposition. *Earth and Planetary Science Letters*, **72**, 433–439.

Kusaba, K., Yagi, T., Kikuchi, M. and Syono, Y. (1986) Structural conditions on the mechanism of the shock-induced zircon to scheelite transition in $ZrSiO_4$. *Journal of Physics and Chemistry of Solids*, **47**, 675–679.

Leroux, H., Reimold, W.U., Koeberl, C., Hornemann, U. and Doukhan, J.C. (1999) Experimental shock deformation in zircon: a transmission electron microscopic study. *Earth and Planetary Science Letters*, **169**, 291–301.

Liu, L.G. (1979) High-pressure phase transitions in baddeleyite and zircon, with geophysical implications. *Earth and Planetary Science Letters*, **44**, 390–396.

Mashimo, T., Nagayama, K. and Sawaoka, A. (1983) Shock compression of zirconia ZrO_2 and zircon $ZrSiO_4$ in the pressure range up to 150 GPa. *Physics and Chemistry of Minerals*, **9**, 237–247.

Meldrum, A., Zinkle, S.J., Boatner, L.A. and Ewing, R.C. (1998) A transient liquid-like phase in the displacement cascades of zircon, hafnon and thorite. *Nature*, **395**, 56–58.

Miotello, A. and Kelly, R. (1997) Revisiting the thermal-spike concept in ion-surface interactions. *Nuclear Instruments and Methods in Physics Research B*, **122**, 458–469.

Nasdala, L., Irmer, G. and Wolf, D. (1995) The degree of metamictization in zircon: a Raman spectroscopic study. *European Journal of Mineralogy*, **7**, 471–478.

Nasdala, L., Wenzel, M., Vavra, G., Irmer, G., Wenzel, T. and Kober, B. (2001) Metamictisation of natural zircon: accumulation versus thermal annealing of radioactivity-induced damage. *Contributions to Mineralogy and Petrology*, **141**, 125–144.

Ono, S., Tange, Y., Katayama, I. and Kikegawa, T. (2004) Equations of state of $ZrSiO_4$ phases in the upper mantle. *American Mineralogist*, **89**, 185–188.

Palenik, C.S., Nasdala, L. and Ewing, R.C. (2003) Radiation damage in zircon. *American Mineralogist*, **88**, 770–781.

Reid, A. and Ringwood, A.E. (1969) Newly observed high pressure transformations in Mn_3O_4, $CaAl_2O_4$, and $ZrSiO_4$. *Earth and Planetary Science Letters*, **6**, 205–208.

Reimold, W.U., Lerouc, H. and Gibson, R.L. (2002) Shocked and thermally metamorphosed zircon from the Vredefort impact structure, South Africa: a transmission electron microscopic study. *European Journal of Mineralogy*, **14**, 859–868.

Ríos, S. and Boffa-Ballaran, T. (2003) Microstructure of radiation-damaged zircon under pressure. *Journal of Applied Crystallography*, **36**, 1006–10012.

Salje, E.K.H., Chrosch, J. and Ewing, R.C. (1999) Is metamictization a phase transition? *American Mineralogist*, **84**, 1107–1116.

Scott, H.P., Williams, Q. and Knittle, E. (2000) Infrared spectra of the zircon and scheelite polymorphs of $ZrSiO_4$ to 26 GPa. Pp. 521–524 in: *High Pressure Science and Technology: Proceedings of the XVII AIRAPT Conference* (M.H. Manghnani, W. Nellis and M. Nicol, editors).

Scott, H.P., Williams, Q. and Knittle, E. (2002) Ultralow compressibility silicate without highly coordinated silicon. *Physical Review Letters*, **88**, art. no. 015506.

Stöffler, D. and Langenhorst, F (1994) Shock metamorphism of quartz in nature and experiment: I. Basic observation and theory. *Meteoritics*, **29**, 155–181.

Stubican, V.S. and Roy, R. (1963) Relation of equilibrium phase-transition pressure to ionic radii. *Journal of Applied Physics*, **34**, 1888–1890.

Trachenko, K., Dove, M.T. and Salje, E.K.H. (2002) Structural changes in zircon under α-decay irradiation. *Physical Review B*, **65**, art.18102(R).

van Westrenen, W., Frank, M.R., Hanchar, J.M., Fei, Y.W., Finch, R.J. and Zha, C.S. (2004) In situ determination of the compressibility of synthetic pure zircon ($ZrSiO_4$) and onset of the zircon–reidite phase transition. *American Mineralogist*, **89**, 197–203.

Weber, W.J., Ewing, R.C. and Lutze, W. (1996) Performance assessment of zircon as waste form for excess weapons plutonium under deep borehole burial conditions. *Materials Research Society Symposium Proceedings*, **412**, 25–32.

Weber, W.J., Ewing, R.C., Catlow, C.R.A., de la Rubia, T.D., Hobbs, L.W., Kinoshita, C., Matzke, H., Motta, A.T., Nastasi, M., Salje, E.H.K., Vance, E. R. and Zinkle, S.J. (1998) Radiation effects in crystalline ceramics for the immobilization of high-level waste and plutonium. *Journal of Materials Research*, **13**, 1434–1484.

Wopenka, B., Jolliff, B.L., Zinner, E. and Kremser, D.T. (1996) Trace element zoning and incipient metamictization in a lunar zircon: application of three microprobe techniques. *American Mineralogist*, **81**, 902–912.

Zhang, M. and Salje, E.K.H (2001) Infrared spectroscopic analysis of zircon: Radiation damage and the metamict state. *Journal of Physics: Condensed Matter*, **13**, 3057–3071.

Zhang, M., Salje, E.K.H., Capitani, G.C., Leroux, H., Clark, A.M. and Schlüter, J. (2000*a*) Annealing of α-decay damage in zircon: a Raman spectroscopic study. *Journal of Physics: Condensed Matter*, **12**, 3131–3148.

Zhang, M., Salje, E.K.H., Farnan, I., Graem-Barber, A., Danial, P., Ewing, R.C., Clark, A.M. and Leroux, H. (2000*b*) Metamictization of zircon: Raman spectroscopic study. *Journal of Physics: Condensed Matter*, **12**, 1915–1925

[*Manuscript received 26 March 2004: revised 4 June 2004*]